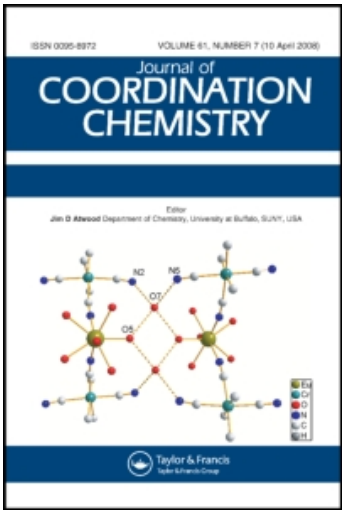

Journal of Coordination Chemistry
Publication details, including instructions for authors and subscription information:
http://www.informaworld.com/smpp/title~content=t713455674

Synthesis, interaction with double-helical DNA and biological activity of new Pt(II) and Pd(II) complexes with phenylglycine

En-Jun Gao[a]; Qiong Wu[a]; Chuan-Sheng Wang[a]; Ming-Chang Zhu[a]; Lei Wang[a]; Hong-Yan Liu[a]; Yun Huang[a]; Ya-Guang Sun[a]
[a] Laboratory of Coordination Chemistry, Shenyang Institute of Chemical Technology, Shenyang, China

First published on: 22 September 2010

To cite this Article Gao, En-Jun , Wu, Qiong , Wang, Chuan-Sheng , Zhu, Ming-Chang , Wang, Lei , Liu, Hong-Yan , Huang, Yun and Sun, Ya-Guang(2009) 'Synthesis, interaction with double-helical DNA and biological activity of new Pt(II) and Pd(II) complexes with phenylglycine', Journal of Coordination Chemistry, 62: 21, 3425 — 3437, First published on: 22 September 2010 (iFirst)
To link to this Article: DOI: 10.1080/00958970903093678
URL: http://dx.doi.org/10.1080/00958970903093678

Journal of Coordination Chemistry
Vol. 62, No. 21, 10 November 2009, 3425–3437

Taylor & Francis
Taylor & Francis Group

Synthesis, interaction with double-helical DNA and biological activity of new Pt(II) and Pd(II) complexes with phenylglycine

EN-JUN GAO*, QIONG WU, CHUAN-SHENG WANG, MING-CHANG ZHU, LEI WANG, HONG-YAN LIU, YUN HUANG and YA-GUANG SUN

Laboratory of Coordination Chemistry, Shenyang Institute of Chemical Technology, Shenyang 110142, China

(*Received 7 December 2008; in final form 3 April 2009*)

The mononuclear palladium(II) (**1**) and platinum(II) (**2**) complexes containing phenylglycine have been synthesized and characterized by elemental analysis, IR spectra, and ^{1}H NMR spectra. The structure of **1** was determined by X-ray diffractometry. The interaction between the complexes and fish sperm DNA (FS-DNA), adenosine-5′-triphosphate (ATP), and adenine (Ade) were investigated by UV absorption spectra, the interaction mode of the complex binding to DNA was studied by fluorescence spectra and viscometry. The results indicate that the two complexes have different binding affinities to DNA, complex **2** > complex **1**. Gel electrophoresis assay demonstrates that the two complexes have the ability to cleave pBR322 plasmid DNA. Cytotoxicity experiments were carried out toward four different cancer cell lines, and **1** shows lower inhibitory efficiency than **2**, consistent with the binding affinities towards DNA.

Keywords: Platinum and palladium complexes; DNA intercalation; Spectroscopy; Cleavage; Cytotoxic activity

1. Introduction

Design of molecules that target DNA sequences has been one of the major challenges in the field of molecular recognition; a more complete understanding of how to target DNA sites with specificity will lead to new chemotherapeutics and a greatly expanded ability to probe DNA and to develop highly sensitive diagnostic agents [1]. Interest in DNA-intercalating ligands as anti-cancer drugs has developed greatly since the clinical success of doxorubicin. DNA-intercalating ligands have diverse structures and capacity to bind tightly but reversibly to DNA by intercalation of a flat aromatic chromophore between the basepairs. Although members of the class show a variety of biological effects, the primary medicinal interest in such ligands has been their potential as anticancer drugs [2, 3]. Small molecules binding to DNA is very important in the development of new therapeutic reagents and DNA molecular probes [4–6]. Binding of platinum complexes to DNA is the key step that sets off the apoptotic pathways in tumor cells [7, 8]. Interest in platinum(II) and palladium(II) complexes have increased

*Corresponding author. Email: ejgao@yahoo.com.cn

Journal of Coordination Chemistry
ISSN 0095-8972 print/ISSN 1029-0389 online © 2009 Taylor & Francis
DOI: 10.1080/00958970903093678

for their potential as antitumor drugs with respect to cisplatin and analogues [9, 10]. Biological experiments performed suggest that DNA is the primary intracellular target of an anticancer complex because the interaction between these molecules and DNA can cause DNA damage in cancer cells, blocking the division of cancer cells and resulting in cell death [11].

This article is devoted to the synthesis and characterization of new Pd(II) (**1**) and Pt(II) (**2**) complexes with phenylglycine acid (scheme 1) and the interaction of these complexes with DNA as explored through spectroscopy and viscometry. Gel electrophoresis assay demonstrates that the complexes have the ability to cleave the pBR 322 plasmid DNA. We have also tested the cytotoxic activities of **1** and **2**.

2. Experimental

2.1. *Materials*

All purchased chemicals were of reagent grade and used without purification unless otherwise noted. Potassium chloride (KCl), hydrochloric acid (HCl), potassium hydroxide (KOH), dimethyl sulfoxide (DMSO), $K_2[PtCl_4]$, and ethidium bromide (EB) are analytical grade, phenylglycine, fish sperm DNA (FS-DNA), adenosine-5′-triphosphate (ATP), and adenine (Ade) are biochemical reagents and used without purification. $K_2[PdCl_4]$ was prepared by reacting $PdCl_2$, KCl, and HCl.

2.2. *Physical measurements*

Elemental analyses (C, H, N) were performed on a Finnigan EA 1112. IR spectra were run as KBr pellets on a Nicolet IR-470. ^{1}H NMR spectra were measured with a Bruker Avance 300 spectrometer operating at 300.13 MHz. UV–Visible (UV–Vis) spectra were recorded on a Shimadzu UV-240. Fluorescence was performed on a Perkin–Elmer LS55 fluorescence spectrofluorometer.

Viscosity tests were performed by keeping the concentration of FS-DNA ([DNA] = 0.1 mM) constant while varying the concentration of the binuclear complex from 5 to 30 μM. Stock solutions of the complexes and DNA were allowed to incubate for 10 min before recording.

For gel electrophoresis experiments, pUC19 plasmid DNA (0.33 μgl L^{-1}) was treated with the Palladium(II) complex in Tris buffer (50 mM Tris–acetate, 18 mM NaCl buffer, pH 7.2), and the contents were incubated for 1 h at room temperature. The samples were electrophoresed for 3 h at 90 V on 0.8% agarose gel in Tris–acetate buffer.

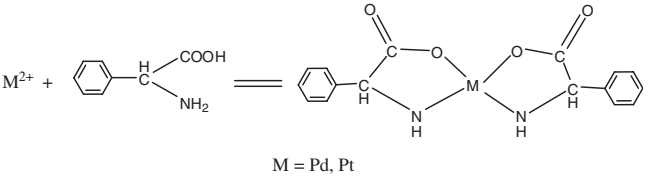

Scheme 1. Preparation of the two complexes.

After electrophoresis, the gel was stained with 1 lg mL^{-1} ethidium bromide and photographed under UV light.

2.3. *Preparation of the complexes and characterization*

$K_2[PdCl_4]$ (water solution, 10 mmol L^{-1}, 10 mL) and phenylglycine (water solution, 10 mmol L^{-1}, 20 mL) were mixed with stirring. Then KOH solution (0.5 mol L^{-1}) was added to adjust pH to 7.12, the solution was filtered to remove a small amount of turbid components, then the turbid components were dissolved with DMSO and allowed to evaporate at room temperature; yellow crystals were obtained 1 week later. Anal. Calcd (%) for $C_{20}H_{28}N_2O_6PdS_2$ (**1**): C, 42.67; H, 5.01; N, 4.97. Found (%): C, 42.67; H, 5.01; N, 4.98. ^{1}H NMR (300 MHz, DMSO-d_6, dppm): 4.65 (singlet (s), 1H, NH_2CHPh), 7.41–7.47 (bm, 5H, Ph). Crystallographic measurements were made on **1** using a Bruker SMART CCD 1000 X-ray single crystal diffractometer. The structure was confirmed and refined with SHELXS [12] and SHELXL [13].

$K_2[PtCl_4]$ (water solution, 10 mmol L^{-1}, 10 mL) and phenylglycine (water solution, 10 mmol L^{-1}, 20 mL) were mixed with stirring and KOH (0.5 mol L^{-1}) added to adjust pH to 5.66, the clear solution was allowed to evaporate at room temperature and some solid power was obtained several weeks later. Anal. Calcd (%) for $C_{20}H_{28}N_2O_6PtS_2$ (**1**): C, 36.82; H, 4.33; N, 4.32. Found (%): C, 36.86; H, 4.33; N, 4.30. ^{1}H NMR (300 MHz, DMSO-d_6, d ppm): 4.75 (singlet (s), 1H, NH_2CHPh), 7.39–7.48 (bm, 5H, Ph).

2.4. *Cytotoxicity assay*

The cell lines used in this experiment were maintained in a RPMI-1640 medium supplemented with 10% (v/v) heat inactivated fetal bovine serum, 2 mmol L^{-1} of glutamine, 100 U mL^{-1} of penicillin, and 100 lg mL^{-1} of streptomycin in a highly humidified atmosphere of 95% air with 5% CO_2 at 37°C.

The growth inhibitory effect of metal complexes on the HeLa cells, the Hep-G2 cells, the KB cells, and the AGZY-83a cells were measured by the microculture tetrazolium [3-(4,5-dimethylthiazol-2-yl)-2,5-diphenyltetrazolium bromide, MTT] assay [14]. In brief, cells were seeded into a 96-well culture plate at 2×10^5 cells per well in a 100 lL culture medium. After incubation for 24 h, cells were exposed to tested complexes of serial concentrations. The complexes were dissolved in DMF and diluted with RPMI 1640 or DMEM to the required concentrations prior to use (0.1% DMF final concentration). The cells were incubated for 24 h and 72 h, followed by addition of 20 lL MTT solution (5 mg mL^{-1}) to each cell and further cultivation for 4 h. The media with MTT were removed and 100 lL DMSO was added to dissolve formazan crystal for 30 min at room temperature. The absorbance of each cell at 450 nm was determined by analysis with a microplate spectrophotometer. The IC_{50} values were obtained from the results of quadruplicate determinations of at least three independent experiments.

In another trial the effect on cell growth of the two complexes and cisplatin were studied by culturing the cells in medium alone for 24 h, followed by 48 h treatment with 5 lM sample solution. The viable cells remaining at the end of treatment were determined by MTT assay and calculated as % of control, treated with DMSO alone under similar conditions.

3. Results and discussion

3.1. *X-ray structure of 1*

The crystal structure of **1** was determined by X-ray crystallography. The structure belongs to the orthorhombic system with space group $P2_12_12$, $a = 14.736(4)$ Å, $b = 14.809(5)$ Å, $c = 5.6813(17)$ Å, $\alpha = \beta = \gamma = 90.00°$. Space stacking structure of **1** with its numbering scheme is shown in figure 1; selected bond lengths and angles are presented in the caption. Crystallographic data and structure refinement of **1** are summarized in table 1. The unit cell is built up by four [Pd (L-Phgly)$_2$] parts and four crystalyzed DMSO molecules. All Pd(II) ions are four coordinate and each is bound to N, N, O, and O coming from two phenylglycine ligands, forming a distorted quadrangular geometry. The N(1)#1–Pd(1)–O(1) bond angle is 176.32(12)° and the N(1)–Pd(1)–O(1), (1)#1–Pd(1)–O(1)#1, O(1)–Pd(1)–O(1)#1, and N(1)–Pd(1)–N(1)#1 bond angles deviate from 90°, suggesting a severe distortion in the Pd(II) quadrangle.

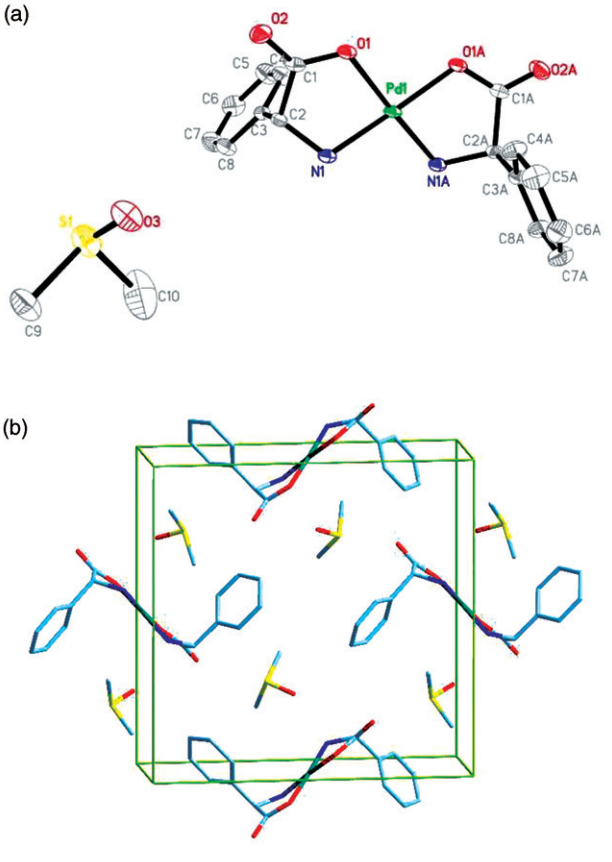

Figure 1. (a) The crystal structures of **1**. (b) Space stacking structure of **1** (H atoms omitted for clarity). Selected bond lengths (nm) and angles (°) for **1**: Pd1–N1 2.035(3), Pd(1)–N(1)#1 2.035(3), Pd1–O1 2.060(3), Pd(1)–O(1)#1 2.060(3), N(1)–Pd(1)–N(1)#1 101.53(12), N(1)–Pd(1)–O(1) 81.29(11), N(1)#1–Pd(1)–O(1) 176.32(12), N(1)–Pd(1)–O(1)#1 176.31(12), N(1)#1–Pd(1)–O(1)#1 81.29(11), O(1)–Pd(1)–O(1)#1 96.03(15). Symmetry transformations used to generate equivalent atoms: #1 $-x+2$, $-y+1$, z.

The angle between benzene ring and chelate ring is 89.43°, approaching 90°, appropriate for intercalation to adjacent base pairs of DNA.

3.2. *Absorption spectrum*

Electronic absorption spectroscopy is a common way to investigate interactions of complexes with DNA. A complex binding to DNA through intercalation usually results in hypochromism and red shift, due to intercalation involving a strong stacking interaction between an aromatic chromophore and the base pairs of DNA [15, 16]. The extent of hypochromism in the UV–Vis band is consistent with the strength of intercalative interaction. In the presence of excess complex, all the FS-DNA studied here shows these features: hypochromism and red shift are progressive and concomitant as shown by the isosbestic points maintained until the end of titration. The absorption spectra of FS-DNA, ATP, and Ade in the absence and presence of the two complexes and the results are given in figure 2 and Supplementary Material. There exists two similar bands at 210 and 260 nm in figure 2 and with increasing complex concentrations, the hypochromisms increase up to 9.0% at 258 nm with isosbestic points at 220 and 257 nm for (a); 14.9% at 259 nm with two isosbestic points at 217–220 nm and 271 nm for (b); 23.5% at 260 nm with three isosbestic points at 217, 229, and 267 nm for (c). Hypochromisms for **2** increase up to 12.1% at 260 nm for (a); 15.3% at 259 nm for (b); 16.5% at 260 nm for (c). The presence of isosbestic points till the end of the titrations of the complexes with DNA rules out the presence of species other than the free and the

Table 1. Crystal data and structure refinement for **1**.

CCDC deposit no.	663177
Empirical formula	$C_{20}H_{28}N_2O_6PdS_2$
Formula weight	562.96
Temperature	294(2) K
Wavelength (λ)	0.71073 Å
Crystal system	Orthorhombic
Space group	$P2_12_12$ (no. 18)
Unit cell dimensions (Å, °)	
a	14.736(4)
b	14.809(5)
c	5.6813(17)
α	90
β	90
γ	90
Volume (Å^3), Z	1239.8(6), 2
Calculated density (g cm^{-3})	1.508
F(000)	576
Crystal size (mm^3)	0.18 × 0.12 × 0.10
θ range for data collection (°)	1.95–26.52
Limiting indices	$-15 \le h \le 18$; $-16 \le k \le 18$; $-4 \le l \le 7$
Reflections collected/unique	6899/2547
Refinement method	Full-matrix least-squares on F^2
Data/restraints/parameters	2547/0/143
Goodness-of-fit on F^2	1.044
Final R indices [$I > 2\sigma(I)$]	$R_1 = 0.0348$, $wR_2 = 0.0736$
R indices (all data)	$R_1 = 0.0456$, $wR_2 = 0.0782$
Largest difference peak and hole (e Å^{-3})	0.183 and −0.378

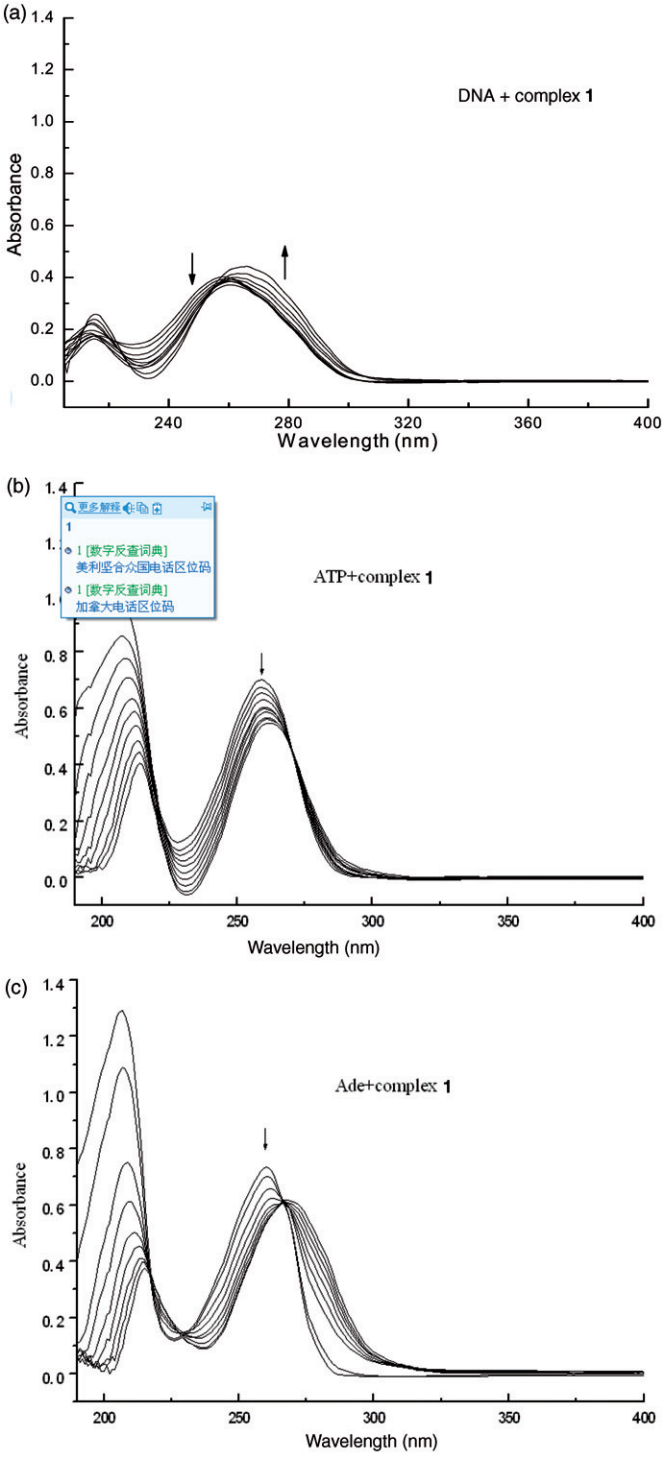

Figure 2. Absorbance spectra of (a) DNA, (b) ATP, and (c) Ade in the absence and presence of increasing amounts of **1**, $C_{DNA} = 50\,\mu M$. Arrow means the increasing of the complex concentration.

intercalated complex. Moreover, it also indicates equilibrium between DNA and metal complexes [17–19]. Based on the extent of hypochromism for Phgly with a small area compared with the co-planar ATP and Ade (figure 2), we can also speculate that the complexes bind to DNA by insertion into adjacent base pairs of the DNA duplex. After intercalation into the base pairs of DNA, the π^* orbital of the intercalated ligand in the complex couples with the π orbital of the base pairs, decreasing the π–π^* transition energy, resulting in hypochromism and bathochromism [20, 21]. From the hypochromisms above, we can compare the binding affinities between the complex with DNA. It affirms that DNA base pairs are the target of the complex interacting with DNA experimentally. Interestingly, there is an absorption enhancement [figure 2(a)], maybe complex concentration is too high and the DNA duplex unfolded [22].

3.3. *Fluorescence spectrum*

An EB replacement assay was carried out to further study the intercalative binding mode between the complexes and DNA. EB is an intercalation reagent that gives a significant increase in fluorescence emission when bound to DNA and its displacement from DNA results in a decrease in fluorescence intensity [23]. The emission spectra of DNA-bound EB in the absence and presence of **1** and **2** are given in figure 3. Addition of the two complexes to DNA incubated with EB solution cause obvious reduction in emission intensities at 605 nm, indicating that the complexes competitively bind to DNA. When the concentration ratios of $[M]/[E]$ attained 10.4 for **1** and 7.92 for **2**, 50% of DNA-bound EB was replaced ($[M]$ is the complex concentration, $[E]$ is the total concentration of EB). According to the classical Stern–Volmer equation [24] $I_0/I = 1 + K_{sq} \times r$, where I_0 and I are the fluorescence intensities in the absence and the presence of the complex, respectively. K_{sq} is a linear Stern–Volmer quenching constant; r is the ratio of total concentration of complex to that of DNA ($[M]/[DNA]$), and in the plot of I_0/I *versus* r. The fluorescence-quenching curve of DNA-bound EB by the two complexes is given in figure 4. The quenching curves illustrate that the complexes bind

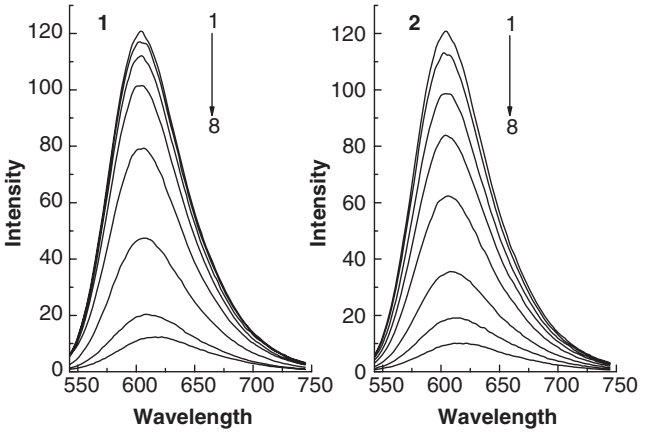

Figure 3. Fluorescence spectra of the binding of EtBr to DNA in the absence (line 1) and presence (lines 2–8) of increasing amounts of the complexes $\lambda_{ex} = 526$ nm, $C_{EtBr} = 1.0\,\mu M$, $C_{DNA} = 5.0\,\mu M$, $C_{M(1-2)}$ (lines 2–8): 1, 2.08, 3.01, 6.855, 20.86, 42.59, 84 (μM).

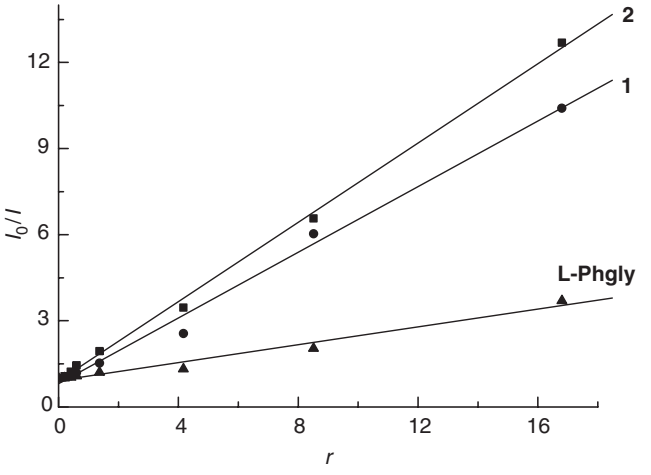

Figure 4. Stern–Volmer quenching plots of **1** and **2** and L-Phgly with the value of slope 0.5722 for **1**, 0.6906 for **2** and 0.1556 for L-Phgly.

to DNA in the sequence of K_{sq} **2** > K_{sq} **1** > L-Phgly, which confirm that reactions of the two complexes and the adjacent DNA base pairs have taken place [25].

Usually a complex, which has bioactivity, will have fluorescence emission to some extent [26]. Emission of the two complexes at 484 nm under excitation wavelength of 376 nm is very weak, but when DNA exists it increases with increasing concentration because DNA can protect the intercalation molecule and enhance the fluorescence intensity. For L-Phgly the phenomenon was not clearly observed (figure 5). The results support the two complexes binding to DNA in an intercalative mode [27].

To further study binding of the complexes to DNA, the fluorescence Scatchard plot experiment was performed. The competition between the complex and EB binding to DNA can be described using the equations [28]:

$$r_E/C_E = (n - r_E)[K_E/(1 + K_M \times C_M)] \quad (1)$$

$$r_M/C_M = (n - r_M)[K_M/(1 + K_E \times C_E)] \quad (2)$$

where r_E, r_M is the ratio of bound EB or the complex to total nucleotide concentration [DNA]: $r_E = ([E] - C_E)/[DNA]$ (1), $r_M = ([M] - C_M)/[DNA]$ (2), C_E and C_M, concentration of free EB and free complex; n, maximum value of r_E and $n = 0.22$ for the linear dichain DNA [29]; K_E and K_M, observed intrinsic binding constant for EB and the complex. In our system EB is the only fluorescent material under the experimental conditions, and fluorescent intensity (F) can be defined as the functions of the concentrations of the intercalative bound ($[E] - C_E$) and the remaining ethidium (C_E):

$$F = K_f \times C_E + K_E([E] - C_E) \quad (3)$$

where K_E, K_f is intrinsic binding constant for EB, determined according to previous literature [30], respectively. When $C_E = [E]$, $F_0 = K_f \times [E]$ (3); $C_E = 0$, $F' = K_E \times [E]$ (4), then C_E is determined from the simultaneous equations (1), (2), and (3):

$$C_E = [(F_0 - F)/(F_0 - F')][E] \quad (4)$$

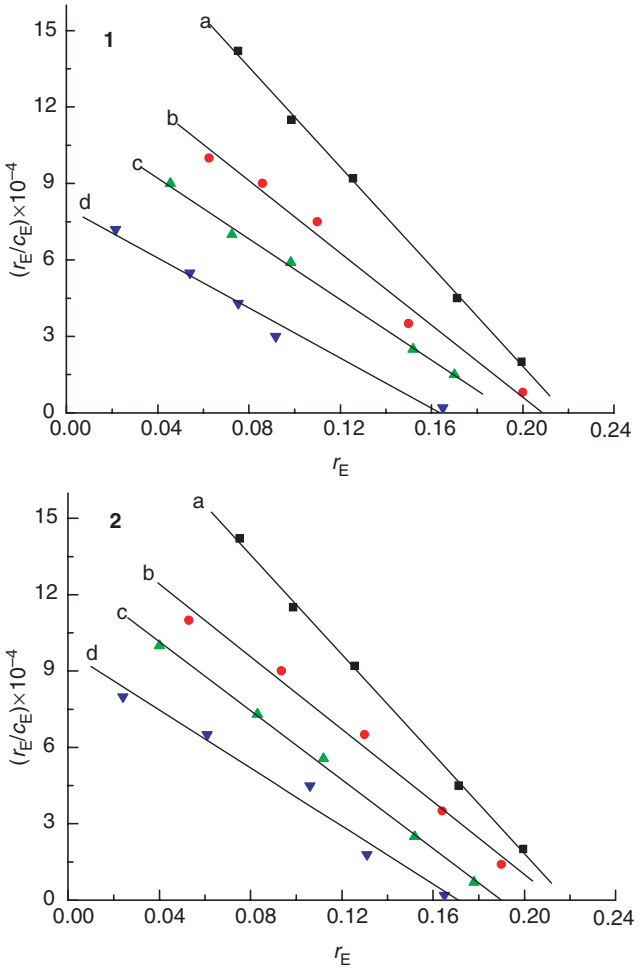

Figure 5. Fluorescence Scatchard plots for binding of EB (0.5–2.5 μM) to DNA in the absence (line a) and presence (lines b–d of **1** and **2**, respectively) of increasing concentration of the Pd and Pt complexes at room temperature, $C_{DNA} = 5\,\mu M$, [EB]/[DNA] = 0.1, 0.2, 0.3, 0.4, 0.5.

From equations (1)–(4), we obtain:

$$r_M = n - r_E - r_E/(K_E \times C_E) \tag{5}$$

$$K_M = [(n - r_E)K_E \times C_E/r_E - 1]/C_M \tag{6}$$

The K_E and n for intercalative EB when complexes of different concentrations are present are listed in table 2. K_E is a linear Scatchard constant dependent on the ratio of the bound concentration of EB to the concentration of DNA and the K_E value is obtained as the slope of r_E/C_E *versus* r_E linear plot [31]. The slope decreases with increase of complex concentration, but no changes in the intercept on the abscissa (n) indicate that the complexes Pd(L-Phgly) and Pt(L-Phgly) interact with DNA via a competitive intercalative binding mode (type A(B) behavior) [29].

3.4. *Viscosity measurements*

Viscosity is sensitive to changes in the length of DNA and is regarded as the least ambiguous means for studying the binding of complexes with DNA in solution and provides strong arguments for intercalative binding [32, 33].

Viscosity measurements were carried out using an Ubbelodhe viscometer maintained at 25.0 ± 0.1°C in a thermostatic water-bath. Flow time was measured with a digital stopwatch. Each sample was measured three times and an average flow time was calculated. Data are presented as $(\eta/\eta_0)^{1/3}$ *versus* binding ratio where η is the viscosity of DNA in the presence of complex and η_0 is the viscosity of DNA alone [34].

The effect of **1** or **2** on the viscosity of FS-DNA is shown in figure 6. Viscosity experiments indicate that both complexes increase the viscosity of FS-DNA, consistent with classical intercalation, validating the UV–Vis spectral titration and EB fluorescence displacement experiments.

3.5. *Gel electrophoresis*

Circular plasmid DNA is ideally suited to probe cleavage events as the DNA exists in a supercoiled state in its native form and converts to a relaxed form upon single strand cleavage, exhibiting an altered migration rate during agarose gel electrophoresis [35, 36]. pBR322 plasmid DNA is used to test the complex (Supplementary Material). In general, this DNA moves on agarose gel under the influence of electrical field, occurring when they are bound to other molecules. Many reports are available for

Table 2. Sample calculation of parameters for fluorescence Scatchard plot of FS-DNA with ethidium in the presence of **1** and **2**.

	1				**2**			
[*M*]/[DNA]	0.000	0.102	0.512	1.090	0.000	0.113	0.496	1.210
$K_E \times 10^{-5}$	9.782	7.540	6.087	5.073	9.782	7.647	7.227	6.306
n	0.218	0.208	0.195	0.164	0.218	0.214	0.190	0.171

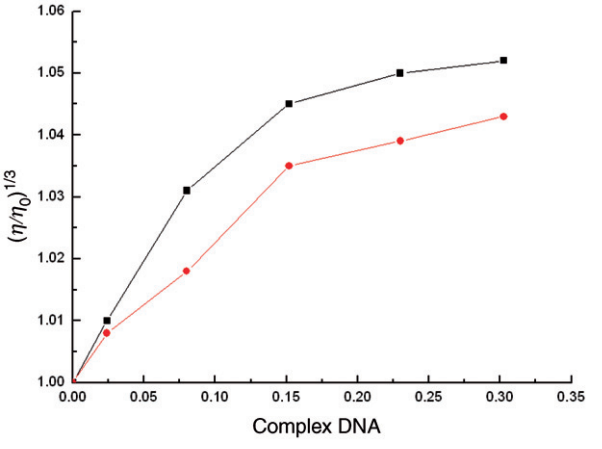

Figure 6. Effect of increasing amounts of **1** (■) and **2** (●) on the relative viscosity of FS-DNA at 25.0 ± 0.1°C.

electrostatic interaction between complex molecules and DNA [37]. Recently, Annaraj *et al.* [38] observed that bipyridine containing complexes interact with DNA due to intercalation of the planar aromatic groups. Palladium(II) and platinum(II) adopt dsp^2 orbital hybridization, forming square planar complexes.

With increase of the complex concentration, intensity of the circular supercoiled DNA (Form I) band decreases, while that of nicked (Form II) increase (lanes 1–5, Supplementary Material). The complexes cleave supercoiled DNA to nicked circular DNA in aerobic condition. Complex **2** exhibits more effective DNA cleavage activity than **1** under comparable experimental conditions, illustrating that gel electrophoretic separations can show different DNA-cleavage efficiencies [39]. Similar observations have also been reported for the other complexes [40, 41].

3.6. *Cytotoxicity* in vitro *study*

The *in vitro* growth inhibitory effects of the two complexes and cisplatin were evaluated in the HeLa, Hep-G2, KB, and AGZY-83a cells. The IC_{50} values are listed in table 3.

Table 3. Cytotoxicity of the complexes and Cisplatin against selected human tumor cells after 24 and 72 h of incubation (data expressed as mean ± SD ($n = 4$)).

Time of incubation	24 h				72 h			
Tumor cells	Hela	Hep-G2	KB	AGZY-83a	Hela	Hep-G2	KB	AGZY-83a
Complex **1**	18 ± 3	6 ± 2	26 ± 5	31 ± 6	5 ± 1	1.8 ± 0.3	6 ± 1	7 ± 1
Complex **2**	9 ± 2	3.1 ± 0.7	14 ± 3	19 ± 4	0.9 ± 0.2	1.2 ± 0.2	3.6 ± 0.5	3.6 ± 0.9
Cisplatin	17 ± 3	7 ± 2	11 ± 2	12 ± 3	0.8 ± 0.2	1.8 ± 0.4	1.6 ± 0.3	2.3 ± 0.6

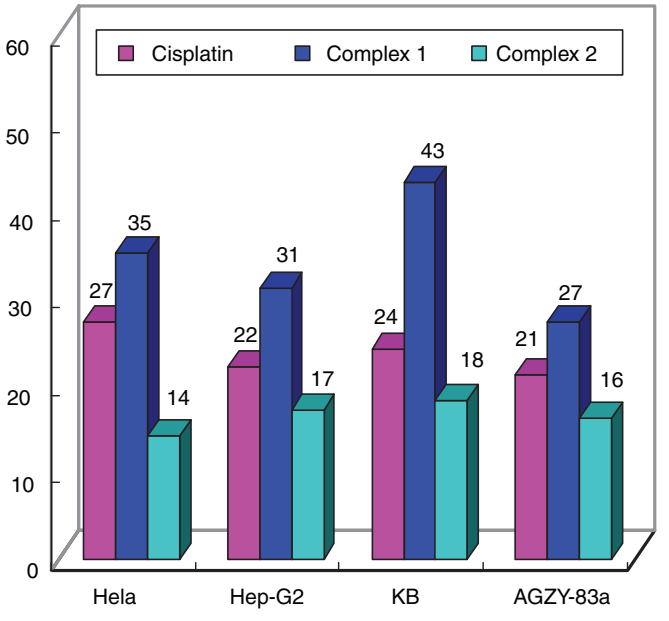

Figure 7. Effect of 10 μg mL^{-1} of the complexes on breast cancer cell viability. All determinations are expressed as percentage of the control (untreated cells).

Figure 7 reveals the effect on cell growth after a treatment period of 48 h with 5 μM concentration. Complex **2** is more active against the cancer cells than **1**. The complexes have higher cytotoxic activity against Hep-G2 cell line than other cell lines. Viability rates by day 3 to less than 50% of the control values were observed for the complexes. The results coincide with IC_{50} values.

4. Conclusions

The complexes Pd-L-Phgly and Pt-L-Phgly were synthesized and characterized. The center metal is located in the center of the plane formed by N, N, O, and O from phenylglycine ligand. DNA binding of the complexes was studied by electronic absorption spectroscopy, fluorescence spectroscopy, and viscometry. The spectroscopic studies indicate interaction of the complexes with Fish-sperm DNA with a strong intercalation mode. The capability of cleavage of pBR 322 DNA by the complexes was investigated using agarose gel electrophoresis and the complexes exhibit efficient DNA cleavage. Cytotoxic activity of **1** shows an inhibitory efficiency slightly lower than **2** on the four cell lines screened, which is in line with their order of affinities towards DNA. The relatively lower toxicity of **1** could be due to decrease in availability caused by its stronger binding with other biomolecules.

Acknowledgements

We gratefully acknowledge the Natural Science Foundation of China (No. 20671064), the Natural Science Foundation of Liaoning Province (No. 20052014), Foundation of Educational Department of Liaoning Province (No. 20060679), Foundation of Liaoning Baiqianwan Talents Program (No. 2008921054), and Phenom Foundation of Liaoning colleges and universities (No. 2007R30).

References

[1] K.E. Erkkila, D.T. Odom, J.K. Barton. *Chem. Rev.*, **99**, 2777 (1999).
[2] A.G. Quiroga, J.M. Perez, E.I. Montero, J.R. Masaguer, C. Alonso, C. Navarro-Ranninger. *J. Inorg. Biochem.*, **70**, 117 (1998).
[3] A.C. Hotze, M. Bacac, A.H. Velders, B.A.J. Jansen, H. Kooijman, A.L. Spek, J.G. Haasnoot, J. Reedijk. *J. Med. Chem.*, **46**, 1743 (2003).
[4] D.B. Hall, R.E. Holmlin, J.K. Barton. *Nature*, **382**, 731 (1996).
[5] L. Mishra, A.K. Yadaw, S. Srivastava, A.B. Patel. *New J. Chem.*, **24**, 505 (2000).
[6] Y.J. Liu, H. Chao, Y.X. Yuan, H.J. Yu, L.N. Ji. *Inorg. Chim. Acta*, **359**, 3807 (2006).
[7] V.M. Gonzalez, M.A. Fuertes, C. Alonso, J. Perez. *Mol. Pharmacol.*, **59**, 657 (2001).
[8] T.W. Hambley. *J. Chem. Soc., Dalton Trans.*, **19**, 2711 (2001).
[9] G. Faraglia, D. Fregona, S. Sitran, L. Giovagnini, C. Marzano, F. Baccichetti, U. Casellato, R. Graziani. *J. Inorg. Biochem.*, **83**, 31 (2001).
[10] E.J. Gao, M.C. Zhu, H.X. Yin, L. Liu, Q. Wu, Y.G. Sun. *J. Inorg. Biochem.*, **102**, 1958 (2008).
[11] H. Zhang, C.S. Liu, X.H. Bu, M. Yang. *J. Inorg. Biochem.*, **99**, 1119 (2005).
[12] G.M. Sheldrick. *SHELXS-97, Program for the Solution of Crystal Structures*, University of Gottingen, Germany (1997).

[13] G.M. Sheldrick. *SHELXL-97*, *Program for the Refinement of Crystal Structures*, University of Gottingen, Germany (1997).
[14] M.C. Alley, S.D.A. Cudiero, A. Monks, H.M.L. Ursey, M.J. Czerwinski, D.L. Fine, B.J. Abbott, J.G. Mayo, R.H. Shoemaker, M.R. Boyd. *Cancer Res.*, **48**, 589 (1988).
[15] J.K. Barton, A. Danishefsky, J. Goldberg. *J. Am. Chem. Soc.*, **106**, 2172 (1984).
[16] E.J. Gao, Y.G. Sun, Q.T. Liu, L.Y. Duan. *J. Coord. Chem.*, **59**, 1295 (2006).
[17] A.M. Pyle, J.P. Rehmann, R. Meshoyrer, C.V. Kumar, N.J. Turro, J.K. Barton. *J. Am. Chem. Soc.*, **111**, 3051 (1989).
[18] H.M. Torshizi, T.S. Srivastava, C.S.J. Havan, M.P. Chitnis. *J. Inorg. Biochem.*, **48**, 1163 (1992).
[19] E.J. Gao, S.M. Zhao, Q.T. Liu, R. Xu. *Acta Chim. Sinica*, **62**, 593 (2004).
[20] A.K. Paul, T.S. Srivastava, S.J. Chavan, M.P. Chitnis, S. Desai, K.K. Rao. *J. Inorg. Biochem.*, **61**, 179 (1996).
[21] E.J. Gao, S.M. Zhao, D. Zhao, Q.T. Liu. *Chin. J. Chem.*, **23**, 54 (2005).
[22] T. Shen, J.Y. Wang. *Biochemistry*, p. 350, Higher Education Publishing Company, China (1989).
[23] G.S. Son, J.A. Yeo, M.S. Kim, S.K. Kim, A. Holmen, B. Akerman, B. Norden. *J. Am. Chem. Soc.*, **120**, 6451 (1998).
[24] J.R. Lakowicz, G. Webber. *Biochemistry*, **12**, 4161 (1973).
[25] H. Arakawa, R. Ahmad, M. Naoui, H.A. Tajmir-Riahi. *J. Biol. Chem.*, **274**, 10150 (2000).
[26] J.Z. Wu, L. Wang, G. Yang, T.X. Zeng, L.N. Ji. *Chem. J. Chin. Univ.*, **17**, 1010 (1996).
[27] X.H. Zou, B.H. Ye, H. Li, J.G. Liu, Y. Xiong, L.N. Ji. *Dalton. Trans.*, 1423 (1999).
[28] E.J. Gao, K.H. Wang, X.F. Gu, Y. Yu, Y.G. Sun, W.Z. Zhang, H.X. Yin, Q. Wu, M.C. Zhu, X.M. Yan. *J. Inorg. Biochem.*, **101**, 1404 (2007).
[29] M. Chien, A.P. Grollman, S.B. Horwitz. *Biochemistry*, **16**, 3641 (1977).
[30] M. Howe-Grant, K.C. Wu, W.R. Bauer, S.J. Lippard. *Biochemistry*, **15**, 4339 (1976).
[31] G. Scatchard, N.Y. Ann. *Acad. Sci.*, **51**, 660 (1949).
[32] S. Satyanarayana, J.C. Dabrowiak, J.B. Chaires. *Biochemistry*, **31**, 9319 (1992).
[33] L.F. Tan, X.H. Liu, H. Chao, L.N. Ji. *J. Inorg. Biochem.*, **102**, 1790 (2007).
[34] M. Cusumano, M.L.D. Piereo, A. Giannetto. *Chem. Commun.*, **101**, 56 (1996).
[35] A.A. Holder, S. Swavey, K.J. Brewer. *Inorg. Chem.*, **43**, 303 (2004).
[36] Y. Jin, M.A. Lewis, N.H. Gokhale, E.C. Long, J.A. Cowan. *J. Am. Chem. Soc.*, **129**, 8353 (2007).
[37] F. Huq, H. Tayyem, P. Beale, J.Q. Yu. *J. Inorg. Biochem.*, **101**, 30 (2007).
[38] J. Annaraj, S. Srinivasan, K.M. Ponvel, P.K. Athappan. *J. Inorg. Biochem.*, **99**, 669 (2005).
[39] J. Qian, W. Gu, H. Liu, F.X. Gao, L. Feng, S.P. Yan, D.Z. Liao, P. Cheng. *Dalton Trans.*, **10**, 1060 (2007).
[40] F.B.A. El Amrani, L. Perello, J.A. Real, M. Gonzalez-Alvarez, G. Alzuet, J. Borras, S. Garcıa-Granda, J. Montejo-Bernardo. *J. Inorg. Biochem.*, **100**, 1208 (2006).
[41] S.C. Jose, E.C. Eduardo, E. Javier, S.G.T. Marıa, M. Luz Perez-Paralle, A. Sanchez, A. Sanchez-Gonzalez, S. Jose, A. Touceda. *J. Inorg. Biochem.*, **102**, 33 (2008).